minerals

MDPI

Article

Using Process Mineralogy as a Tool to Investigate Blending Potential of the Pentlandite-Bearing Ores at the Nkomati Ni Mine in South Africa

Thomas Dzvinamurungu [1,2], Derek Hugh Rose [1], Ngonidzashe Chimwani [3] and Fanus Viljoen [1,*]

[1] Department of Geology, University of Johannesburg, Auckland Park, Kingsway Campus, P.O. Box 524, Johannesburg 2006, South Africa; dzvinamurungut@staff.msu.ac.zw (T.D.); derekr@uj.ac.za (D.H.R.)
[2] Department of Geosciences, Midlands State University, Private Bag 9055, Senga Road, Gweru, Zimbabwe
[3] Department of Mining, University of South Africa (UNISA), Florida Campus, Private Bag X6, Johannesburg 1710, South Africa; ngodzazw@gmail.com
* Correspondence: fanusv@uj.ac.za

Abstract: The mineralogy and texture of Ni-sulfide ores at the Nkomati nickel mine are highly variable, and this results in often erratic nickel recovery at the mine. The variability of the ore presents an opportunity to study the influence of grind size on the flotation-based recovery of Ni in highly heterogeneous sulfide ores, which would be applicable to this ore type at many other mines worldwide. In view of this, a process mineralogy investigation was conducted on thirteen mineralogically and texturally different nickel-sulfide ores from the Nkomati Nickel Mine, with a view on the influence of grind size on the flotation performance of pentlandite. Ore types presented include medium- and high-grade variants of the bleb, disseminated, massive, semi-massive, and net-textured sulfide ores of the Main Mineralized Zone (MMZ), as well as disseminated chromite-rich nickel sulfide ore and massive chromitite ore of the Peridotitic Chromitite Mineralized Zone (PCMZ). Laboratory scale metallurgical test work, comprising of sequential grinding and bench-top flotation testing of the ores, was conducted in combination with quantitative mineralogical investigation of the flotation feed and associated flotation products, using a FEI 600F Mineral Liberation Analyzer. The ore types under consideration require a variety of grind sizes (i.e., milling times) in order to attain optimal recovery of nickel through flotation. This is predominantly controlled by ore texture, and also partly by the abundance of the major constituent minerals in the ore, being pyroxenes, base metal sulfides, and chromite. Liberation of pentlandite is directly correlated with grind size (milling time), which is also positively correlated with the level of nickel recovery through flotation. A grind size of P80 at 75 µm results in the highest concentrate nickel grades of 7.5–8.1% in the PCMZ ores' types which is the current grind for the PCMZ ores at Nkomati. A grind size of P77 at 75 µm yields the best overall pentlandite liberation, Ni recoveries of 84–88% and grades of 5.3–5.6% in the MMZ ores. This holds the potential to produce the best overall pentlandite liberation, nickel grades, recoveries from blending the MMZ and PCMZ ore types, and milling the composite ore at a target grind of P80 at 75 µm.

Keywords: ore texture; grind sizes; milling; liberation analysis; pentlandite; flotation; flotation kinetics; recovery

Citation: Dzvinamurungu, T.; Rose, D.H.; Chimwani, N.; Viljoen, F. Using Process Mineralogy as a Tool to Investigate Blending Potential of the Pentlandite-Bearing Ores at the Nkomati Ni Mine in South Africa. *Minerals* **2022**, *12*, 649. https://doi.org/10.3390/min12050649

Academic Editor: Pura Alfonso

Received: 7 April 2022
Accepted: 18 May 2022
Published: 20 May 2022

1. Introduction

Nickel is a ferromagnetic transition metal, markedly resistant to oxidation and corrosion. It is malleable, ductile, and has superior strength and corrosion resistance even at high temperatures and it provides an excellent base for developing specialized alloys, such as stainless steel. Nickel and nickel alloys are non-ferrous metals with high strength and toughness, excellent corrosion resistance, and superior elevated temperature properties.

This makes nickel a highly versatile material that alloys with most metals for a wide variety of industries, such as aircraft gas turbines, steam turbines in power plants, and is used intensively in the energy and nuclear power industries [1].

Economically important ore types hosting nickel are limonite (Fe-hydroxide) and garnierite (Ni-laterite) type ores, as well as the sulfide minerals, pentlandite ((Ni, Fe)$_9$S$_8$), and pyrrhotite (ranging in composition from FeS to Fe$_7$S$_8$, and in which some of the iron may be replaced by nickel). Magmatic sulfide deposits such as Norilsk in Russia [2], Sudbury in Canada [3,4], and Kambalda in Australia [5]), as well as laterite deposits (e.g., those occurring in Cuba, New Caledonia, and Indonesia [6,7]), account for the bulk of nickel production world-wide. Magmatic sulfide deposits host about 40% of the global nickel resource, and currently are the source of more than 50% of the world's nickel supply, while laterite deposits are host to approximately 70% of the world's nickel resource [8].

Pentlandite is generally found within the lower margins of mineralized layered intrusions, for example, in the troctolite of the Voisey's Bay intrusive complex in Canada, and in the gabbro of the Duluth Complex of North America and the Bushveld Igneous Complex in South Africa [3,9–11]. The nickel sulfide deposits (and minerals) often also contain cobalt, copper, and platinum-group metals. Increasing demand for nickel in the stainless-steel manufacturing industry and the continuous depletion of nickel resources, compounded by high processing costs, have resulted in substantial increases in the price of nickel, and this has precipitated much interest in the optimization of the nickel recovery processes [12].

This paper focuses on pentlandite in ore from the Nkomati Nickel Mine, which is located in the Uitkomst Complex in South Africa [11,13–17]. Nkomati is the only primary nickel producing mine in South Africa, with pentlandite being the main nickel-bearing mineral. Two ore horizons are being mined for nickel, these being the Main Mineralized Zone (MMZ) as well as the Peridotitic Mineralized Zone (PCMZ), with each of these characterized by a variety of ore textures and mineralogy [11,18,19]. The ore types of the MMZ ores are comprised of: high- and medium-grade bleb (Bleb_HG and Bleb_MG); disseminated (Dis_HG and Dis_MG); massive (MS_HG and MS_MG); semi-massive (SMS_HG and SMS_MG); and net-textured (Net_HG and Net_MG) varieties. In contrast, the ore types of the PCMZ consist of high- and medium-grade variants of disseminated chromite-rich nickel sulfide ores (PCMZ_HG and PCMZ_MG), as well as massive chromitite ore (MCHR). Accepted practice at Nkomati is to mill the MMZ sulfide ores at a grind of 67% passing 75 micron (i.e., P67 at 75 µm) and P80 at 75 µm (PCMZ ore horizon), followed by a separate bulk sulfide flotation of the two ore types.

The liberation of sulfides through milling, and their efficient recovery through bulk sulfide flotation concentration, are closely related to the ore mineralogy and ore texture, which often pose processing problems for complex ore types [20]. Textural analysis of the ore minerals provides predictive liberation information and also acts as a basis for an economic evaluation of a technological scheme for mineral processing [21,22]. Therefore, the optimum liberation and recovery of valuable minerals in texturally complex ores require varying degrees of grinding to optimize mineral liberation and energy consumption of the mining operation. This is achieved by having the ore milled not finer than the optimum liberation required; and to ensure that the liberated minerals are not ground finer than absolutely necessary, as that overgrinding will further inhibit their recovery during flotation [10,23].

The processing philosophy at the Nkomati mine is to blend the different sulfide ore textural varieties from each ore horizon into a 'required' run-of-mine mill feed, which is then processed further to ultimately obtain a bulk flotation concentrate [24]. However, ore blending could lead to synergistic and antagonistic effects from the individual ore types, of varying mineralogy and texture, during mineral processing, while the overall contribution of a specific ore type to overall processing efficiency may be masked [20,25–27].

The influence of ore mineralogy and texture on the recovery of Ni from the MMZ ore horizon at Nkomati (milled at a grind size of P67 at 75 µm) was studied before (but excluded the effect of varying grind size) [20], while the PCMZ remained unstudied. Hence,

the aim of the present study is to assess the impact of variable grind size on flotation performance [25,26,28–34] for the MMZ and the PCMZ ore horizons. This objective is achieved by conducting laboratory-scale sequential grinding, bench-top flotation, and quantitative mineralogical investigation of the flotation feed and flotation products [28,33,34]. Although commonly conducted in-house by the various mining companies, published case studies are comparatively rare, and hence the results of the present study should also be of use to other mines world-wide where nickel is recovered from sulfide ores of varying ore mineralogy and texture.

2. Technical Background

The geology of the Uitkomst Complex and mineralization at Nkomati Nickel Mine have been well documented by [11,13–19]. This study focuses primarily on the MMZ and the PCMZ orebodies that, at the time of undertaking this study, were being exploited at the Nkomati mine (the mine is currently under care and maintenance). These two orebodies are characterized by varying sulfide textures, which include disseminated, net-textured, and massive varieties. There are also varying degrees of alteration and oxidation in certain areas of the orebodies, with the development of a variety of secondary silicate and oxide minerals [11,13,14,16,17]. The mine feed cut-off grade is 0.3% Ni for the MMZ ores and the target grind employed at the mine is 67 wt% passing 75 µm, while the mine cut-off grade of the PCMZ ores is 0.25% Ni with a target grind of 80 wt% passing 75 µm. Metal recovery is accomplished through froth flotation [18,19].

3. Sampling and Methodology

3.1. Sampling

Thirteen representative samples were collected from ore stockpiles at the Nkomati mine for petrographic study, the acquisition of quantitative mineralogical data using an automated SEM-based platform, as well as laboratory-scale metallurgical test work which included milling and flotation. The samples were hand-sorted according to sulfide texture types. Following the approach documented by [19], ten samples, about 12 kg each, were collected from the MMZ ore stockpiles (high- and medium-grade ore stockpiles) and three samples were collected from the PCMZ ore stockpiles, respectively. The ten samples from the MMZ comprised high- and medium-grade variants of the bleb (denoted by Bleb_HG for the high-grade variant and Bleb_MG for the medium-grade variant), disseminated (Dis_HG and Dis_MG), massive (MS_HG and MS_MG), semi-massive (SMS_HG and SMS_MG), and net-textured (Net_HG and Net_MG) sulfide ores. The three samples from the PCMZ ore stockpiles consisted of high- and medium-grade variants of disseminated chromite-rich sulfide ore (denoted by PCMZ_HG for the high-grade variant and PCMZ_MG for the medium-grade variant), and a massive chromitite ore (MCHR).

Each sample was crushed to −2 mm and split using a rotary sample splitter into 6 × 1 kg sample aliquots for milling and flotation, while 75–100 g were submitted for assay, and 3 g aliquots were used to prepare 30 mm resin mounts for mineral liberation analysis (MLA). Three MLA block mounts were prepared for each ore type, per three grind sizes, and were analyzed at the University of Johannesburg. Geochemical analysis was conducted at the Genalysis laboratories in Australia.

3.2. Petrography

Polished thin sections of ore samples from the MMZ and the PCMZ were subjected to petrographic analysis on an Olympus BX51 Optical Microscope, to determine the mineralogy and textural characteristics of the different ore types [35–38].

3.3. Automated Mineralogy

Representative splits of each coarsely crushed (−2 mm) ore type sample (also referred to as unprocessed ore) were mixed with resin and then cast into 30 mm resin molds to set. The 30 mm blocks were polished, coated with carbon, and examined with an FEI 600F MLA

for mineral modal mineralogy, using the GXMAP procedure [39,40]. All analyses were completed at 350× magnification. The samples were also examined for pentlandite grain sizes' distribution, using the SPL_GXMAP procedure.

All of the milled ore feeds, collected from the swirling pulp in the flotation cell prior to flotation, were sieved to −75 + 38 µm in order to exclude any fine materials that may report to the concentrate through entrainment and entrapment, rather than true flotation [41,42]. The −75 + 38 µm fraction most likely contains material that reports to the concentrate by true flotation, while the coarser particles (e.g., >75 µm) and the finer materials (e.g., <38 µm) float poorly [43,44]. Although optimization of the flotation kinetics may still result in the efficient recovery of both fine and coarse particles [45,46], this is not the primary focus of the present contribution. Each of the fractions was split into representative aliquots using a rotary micro riffler, mixed with resin and cast into 30 mm blocks, polished and coated with carbon. These were then examined for pentlandite liberation using SPL_GXMAP.

3.4. Milling

The samples collected for study were subjected to mill tests in order to determine their milling behavior with respect to the rate at which the ore is reduced in size with progressive milling time. This was accomplished using ore which was crushed to −2 mm. A 210 mm diameter steel rod mill, charged with a 1 kg sample aliquot, was utilized, in conjunction with 6 × 25 mm, 8 × 20 mm and 6 × 16 mm mill rods [47]. Prior to milling, 1 kg of crushed quartz [44] was milled in 500 mL water for 15 min, in order to clean the mill. Following disposal of the quartz and rinsing, a 1 kg sample aliquot was then placed in the mill, with 500 mL of water added, in order to produce a slurry comprising of 66% solids by weight. The rotation of the rod mill was set at 61 rpm.

Milling was conducted for 10 min and the grind was determined (as weight % passing 75 µm) by wet sieving and weighing of the milled product after drying in an oven at low temperature (110 °C). The samples were then returned to the mill for a further 15 and 25 min of milling (that is, a total milling time of 50 min), and the size analysis was conducted again for each of these additional milling intervals.

Using the milling rate data thus produced, further milling was conducted on new 1 kg aliquots of each ore type (crushed to −2 mm) for grind sizes of P57, P67, and P77 at 75 µm (MMZ) as well as grind sizes of P70, P80, and P90 at 75 µm (PCMZ).

3.5. Flotation

Laboratory scale flotation testing was conducted using a 2.5 L flotation cell mounted on a Denver laboratory flotation test machine. The milled slurry was made up to 35% solids by adding a further 1.36 L of water. The impeller speed was set at 1100 rpm and the air flow rate was maintained at 7 L/min in all of the tests. A froth depth of 2 cm was maintained, and a scraping depth of 0.5 cm above the slurry level was utilized for the froth collection. Before starting flotation, 65 mL (or about 60 g dry weight) of the swirling pulp in the flotation cell was collected for chemical analysis ('assay') of the flotation feed. Details of the reagents used, additional sequence and conditioning times are as per [19]. The reagents added included primary collector sodium isobutyl xanthate (SIBX), secondary collector Senkol 700, frother Senfroth 200, and depressant Sendep 300. All of the reagents used were supplied by Senmin Chemicals Pty LTD (now known as AECI Mining).

Dosages of 10, 100, 20, and 350 g/t of Senkol 700, SIBX, Senfroth, and Sendep were used, respectively. A volume of 0.01 mL Senkol 700 was added to the mill charge prior to milling, after which the mill charge was then milled to the target grind.

A 10 mL volume of the SIBX was added to the flotation cell while running at 1100 rpm and conditioned for 1 min, followed by 2 mL of Senfroth 200 and a further 2 min of conditioning. A volume of 17.5 mL Sendep 300 was finally added, followed by a further 2 min of conditioning time.

Air flow into the flotation cell was initiated, and concentrates were collected by scraping the froth every 15 s for 1, 3, 10 L and 30 min of cumulative flotation times for each

of the four timed concentrates, respectively. Each feed, concentrate, and tailing sample was dried in an oven at 110 °C, and cooled in air. Concentrate volumes ('mass pulls'; i.e., the flow rate of solids reporting to the concentrate) were determined through weighing. Flotation tests were executed in duplicate for each ore type; with the feed, concentrate, and flotation tailings combined per sample.

The concentrations of Ni and other elements in the feed and tailings were analyzed at the Genalysis Laboratory in Australia [48]. The detection limit of Ni is in the order of 1 ppm (optical emission spectrometry). The recovery of Ni is based on the mass of Ni in the feed, concentrate, and flotation tailings. Concentrate grade is based on the mass of Ni in the concentrate and is expressed as a function of Ni recovered from the flotation feed.

4. Ore Sample Characterization

4.1. Macroscopic Description

Five sulfide ore textures namely, the bleb, disseminated, massive, semi-massive, and net-textures are represented in the ore samples selected from the MMZ ore horizon (Figure 1A–E; Table 1). Two ore textural types comprise the samples from the PCMZ ore horizon, being disseminated chromite-rich sulfide ores, as well as a massive chromite ore (Figure 1F,G; Table 1).

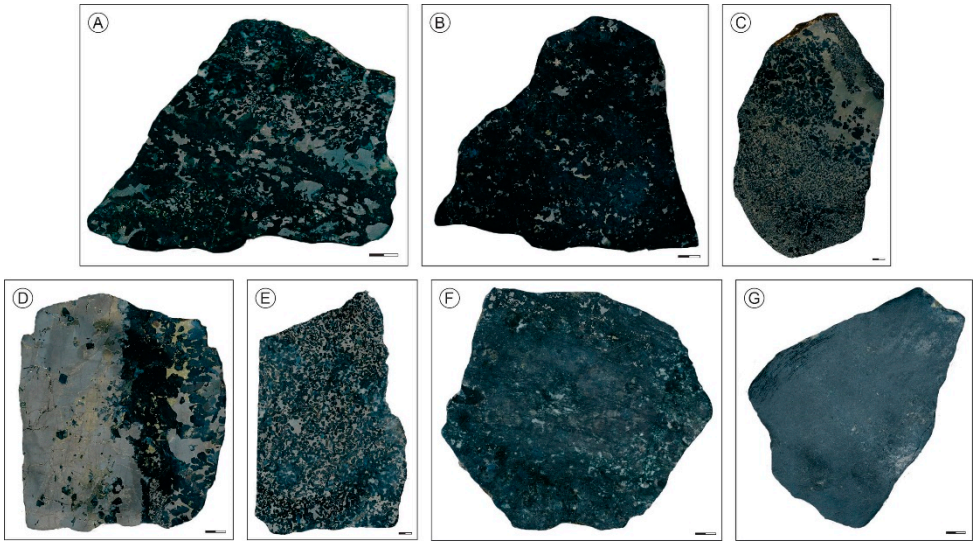

Figure 1. Macroscopic images of the distribution of sulfides (i.e., rock textures) of hand-sized polished rock slabs of ore samples collected from the MMZ (**A**–**E**), as well as the PCMZ (**F**,**G**) ore horizons. Scale bar bottom right = 1 cm.

Table 1. Macroscopic textures of ore types from the MMZ AND PCMZ ore horizons.

Ore Type	Mineralogical Description
Bleb texture sulfide ore (MMZ)	Large composite sulfide grains which are uniformly distributed throughout the rock (Figure 1A).
Disseminated sulfide ore (MMZ)	Sparsely distributed sulfides, with a smaller grain size than those in the bleb sulfide ores (Figure 1B).
Semi-massive sulfide ore (MMZ)	Bleb sulfides, some of which enclose silicates (Figure 1C).
Massive sulfide ore (MMZ)	Large connected sulfide masses, enclosing other minerals in the rock (Figure 1D).
Net-textured sulfide ore (MMZ)	Mesh-like networks of sulfides enclosing other minerals in the rock (Figure 1E).

Table 1. *Cont.*

Ore Type	Mineralogical Description
Disseminated chromite-rich sulfide ore and massive chromitite ore (PCMZ)	These ore types have a comparable mineral assemblage, comprising mainly of chromite, orthopyroxene, clinopyroxene, chlorite, serpentine, and sulfides, but with variable mineral abundances (Figure 1F,G). The disseminated sulfide ore variant (Figure 1F) is characterized by higher abundances of sulfide, and is texturally somewhat coarser, with a lower abundance of chromite compared to the massive chromitite variety (which has the smallest grain size of all of the ore types investigated (i.e., MMZ and PCMZ; Figure 1G). The chromite grains are often surrounded by, and enclosed in, a network of secondary fibrous chlorite and serpentine (Figure 1F,G).

4.2. Microscopic Description

Petrographic features of the ore types are as per Figures 2–6, and Tables 2 and 3.

Table 2. Microscopic (petrographic) descriptions of thin section of the MMZ ores.

Ore Type	Mineralogical and Petrographic Description
High-grade bleb ore (Bleb_HG)	Coarse grains of orthopyroxenes, clinopyroxenes, medium-grained amphiboles, fine-grained chlorite, and large poikilitic plagioclase crystals enclose clinopyroxene, orthopyroxene, and chlorite (Figure 2A,B). The clinopyroxenes and orthopyroxenes are altered along grain boundaries to chlorite. Composite sulfide blebs comprise chalcopyrite, pentlandite, pyrrhotite, and pyrite, which are mainly located on silicate grain boundaries (Figure 2C). Disseminated fine-grained sulfides are seen.
Medium-grade bleb ore (Bleb_MG)	Medium grade ore consists of large crystals of orthopyroxene, clinopyroxene, and plagioclase; and medium to fine-grained crystals of Ca-amphibole, chlorite, and base metal sulfides (Figure 2B–E). Clinopyroxene and orthopyroxene have been altered around the rims to form a spongy texture, comprising mainly of chlorite. Some poikilitic orthopyroxene crystals enclose plagioclase (Pl) grains. SulfideSulfide blebs consist of chalcopyrite, pentlandite, pyrrhotite, and pyrite, and are located along silicate grain boundaries (Figure 2E,F).
High-grade disseminated ore (Dis_HG)	Consists of large crystals of orthopyroxene, clinopyroxene, and amphibole; and fine sulfides. Some of the orthopyroxene and clinopyroxene crystals are fractured, with fractures and grain edges altered to chlorite (Figure 3A,B). Composite sulfide grains comprises of chalcopyrite, pentlandite, pyrrhotite, and pyrite; and are mainly located along silicate grain boundaries (Figure 3C,D).
Medium-grade disseminated ore (Dis_MG)	Consists of fine to medium-grained clinopyroxene, orthopyroxene, and large grains of poikilitic plagioclase enclosing some of the clinopyroxene, hornblende, chlorite, and sulfide. Plagioclase is partially altered to a spongy feature in places, and clinopyroxene is altered along the margins to mainly chlorite (Figure 3E,F).
High-grade massive sulfide ore (MS_HG)	Consists of medium- to fine-grained clinopyroxene and orthopyroxene which have been partially altered to chlorite; with minor oxides present (Figure 4A). Sulfide veining is prevalent in the silicates. Large massive sulfide composites comprise of chalcopyrite, pentlandite, pyrrhotite, and pyrite (Figure 4B,C).
Medium-grade massive sulfide ore (MS_MG)	The ore contains fine-grained orthopyroxenes and clinopyroxenes which are altered, to form mainly chlorite (Figure 4D). Large composite massive sulfides comprise pentlandite, pyrrhotite, and pyrite (Figure 4F). Some of the silicate minerals are enclosed within the massive sulfides, and some of the sulfide minerals are located on silicate grain boundaries.

Table 2. *Cont.*

Ore Type	Mineralogical and Petrographic Description
High-grade semi-massive ore (SMS_HG)	Comprises coarse-grained orthopyroxene and clinopyroxene enclosed within semi-massive sulfides. Orthopyroxene and clinopyroxene are fractured, and altered along the margins to chlorite (Figure 5A–C). Coarse-grained composite sulfides consist of chalcopyrite, pentlandite, pyrrhotite, and pyrite (Figure 5D,E). Some of the small sulfide grains are disseminated within the silicates, and some fill fractures in the silicate minerals to form veins.
Medium-grade semi-massive ore (SMS_MG)	The medium-grade semi-massive ore variant consists of medium-grained orthopyroxene, clinopyroxene and plagioclase; and fine-grained chlorite within the semi-massive sulfides. The large composite sulfide grains comprising chalcopyrite, pentlandite, pyrrhotite and pyrite encloses some of the silicate minerals (Figure 5F).
High-grade net-textured ore (Net_HG)	Consists of coarse to medium grained grains of orthoclase, orthopyroxene, clinopyroxene and hornblende along with secondary calcite. Silicate minerals are often enclosed within networks of sulfides (Figure 6A,B). The composite sulfides comprise chalcopyrite, pentlandite, pyrrhotite and pyrite, which form around silicate grain boundaries (Figure 6C). Oxides are also present enclosed within sulfides, while alteration of sulfide to metal oxides is also seen.
Medium-grade net-textured ore (Net_MG)	Consists of large poikilitic plagioclase crystals that enclose grains of orthopyroxene, clinopyroxene, hornblende, and probable secondary chlorite. Some of the sulfides occur as networks around silicate minerals (Figure 6D,E). Orthopyroxenes and clinopyroxene are often fractured, and the fractures and grain boundaries are altered to chlorite. The composite sulfide grains comprise chalcopyrite, pentlandite, pyrrhotite, and pyrite and some of the sulfides have been replaced by Fe-oxides along grain boundaries (Figure 6F). Finer-grained sulfides are disseminated throughout the silicate matrix.

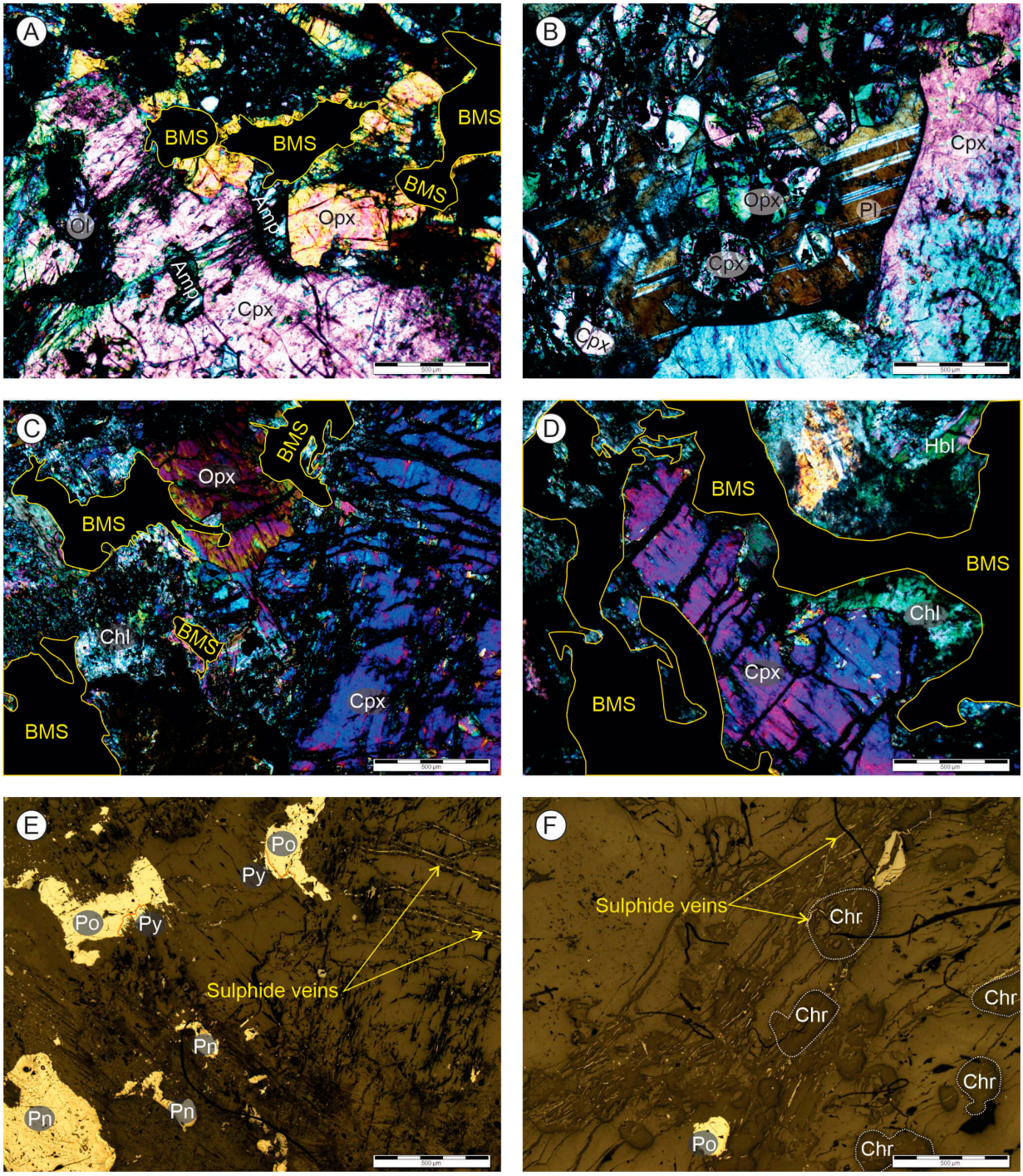

Figure 2. Photomicrographs of the medium-grade and high-grade bleb textured sulfide ores ((**A–D**) transmitted plane polarized light; (**E**,**F**) reflected light). The mineral abbreviations are as follows: amphibole (Amp); chlorite (Chl); clinopyroxene (Cpx); chromite (Chr); glaucophane (Gln); hornblende (Hbl); orthopyroxene (Opx); oxide (Ox); plagioclase (Pl); chalcopyrite (Ccp); pentlandite (Pn); pyrrhotite (Po); pyrite (Py); serpentine (Srp); and talc (Tlc). The scale bar at the bottom right of the images represents 500 μm. BMS = base metal sulfides.

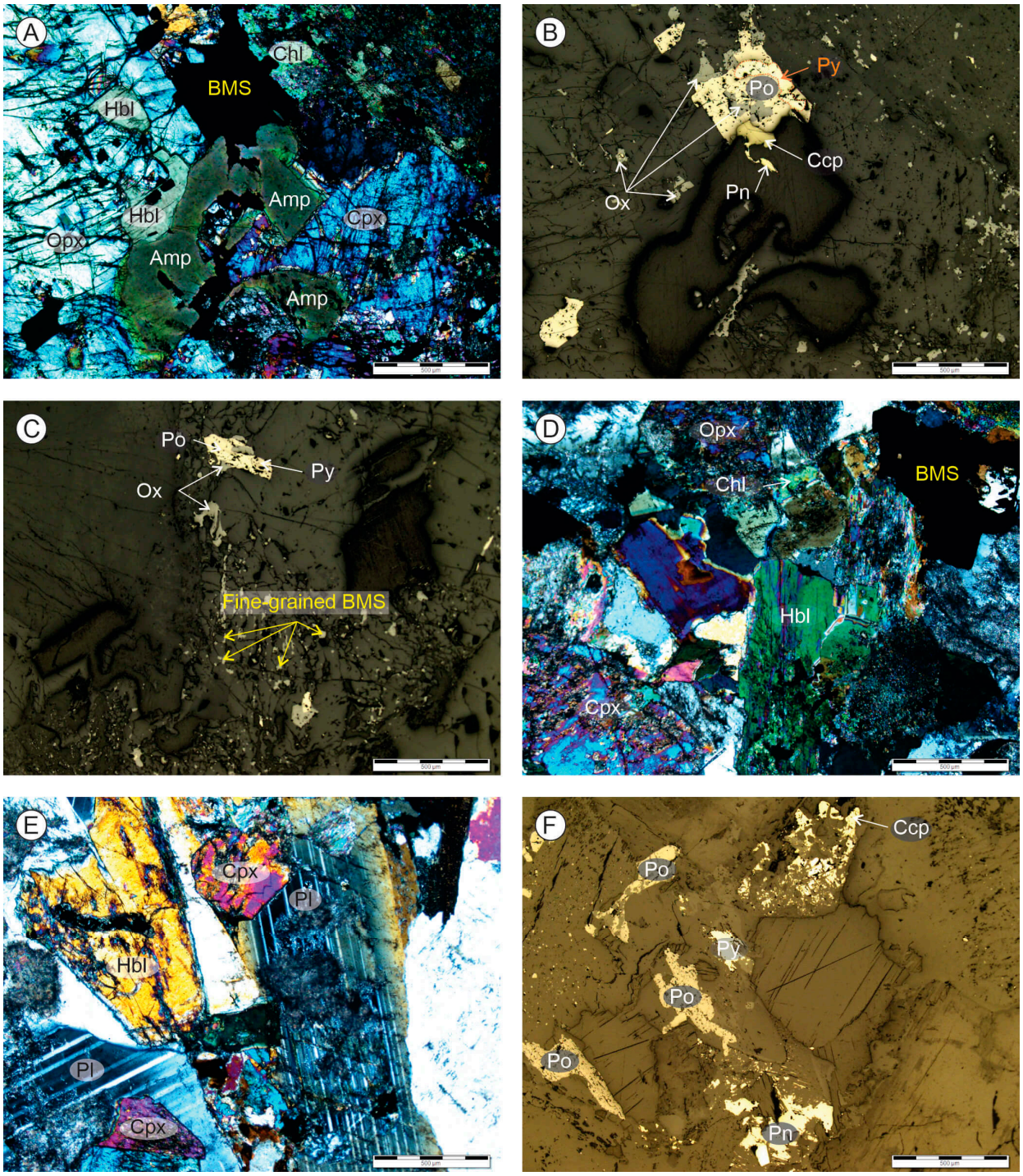

Figure 3. Photomicrographs of the high-grade and medium-grade disseminated sulfide ores showing various silicate (**A**,**D**,**E**) and sulfide (**B**,**C**,**F**) minerals. The scale bar at the bottom right corner of the images represents 500 µm. Refer to Figure 2 for explanation of the mineral abbreviations.

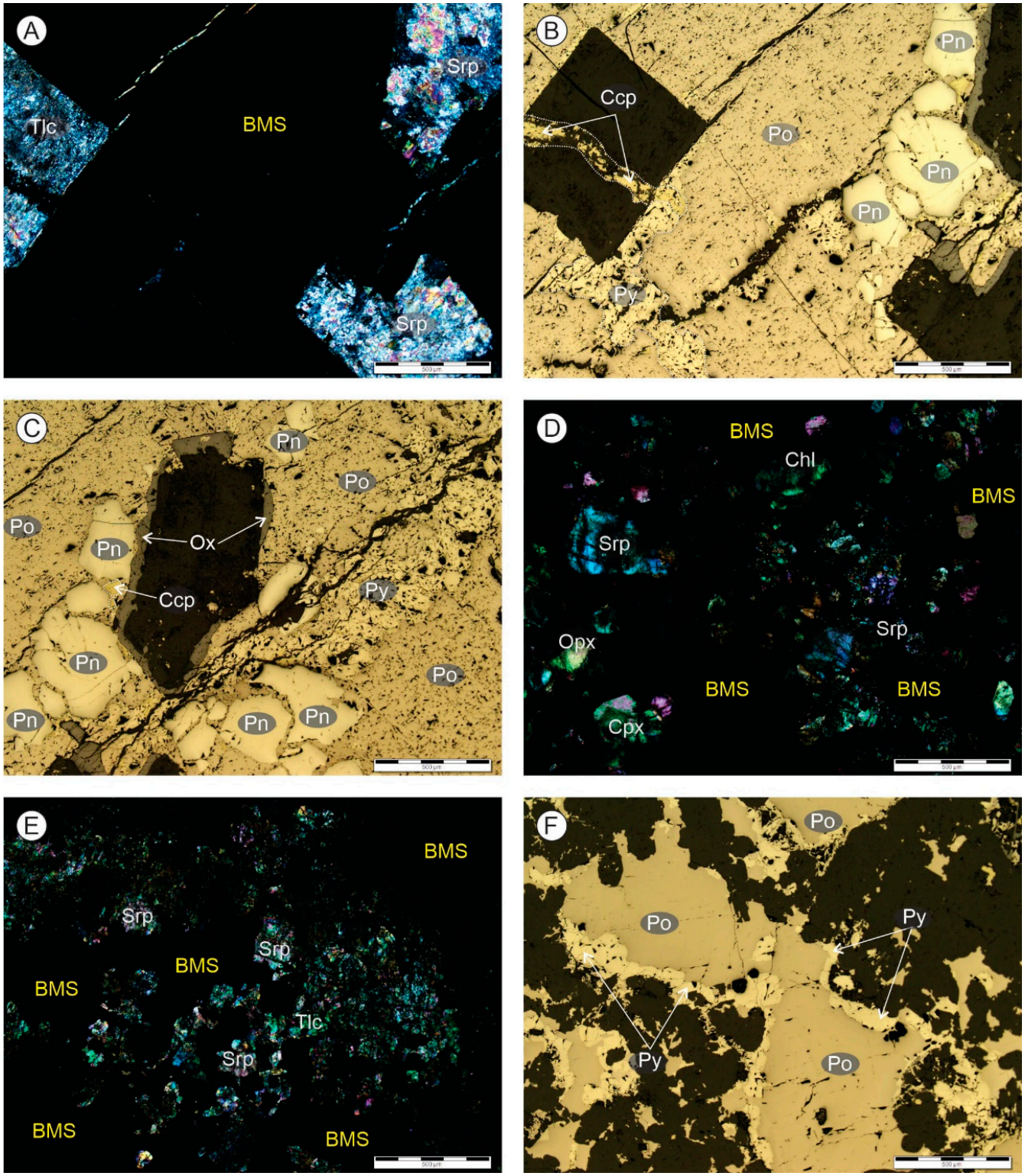

Figure 4. Photomicrographs of the high-grade massive sulfide ores (**A**–**C**) as well as the medium-grade massive sulfide ores (**D**–**F**) show various silicates and composite sulfides. The scale bar at the bottom right corner of the images represents 500 µm. Refer to Figure 2 for explanation of the mineral abbreviations.

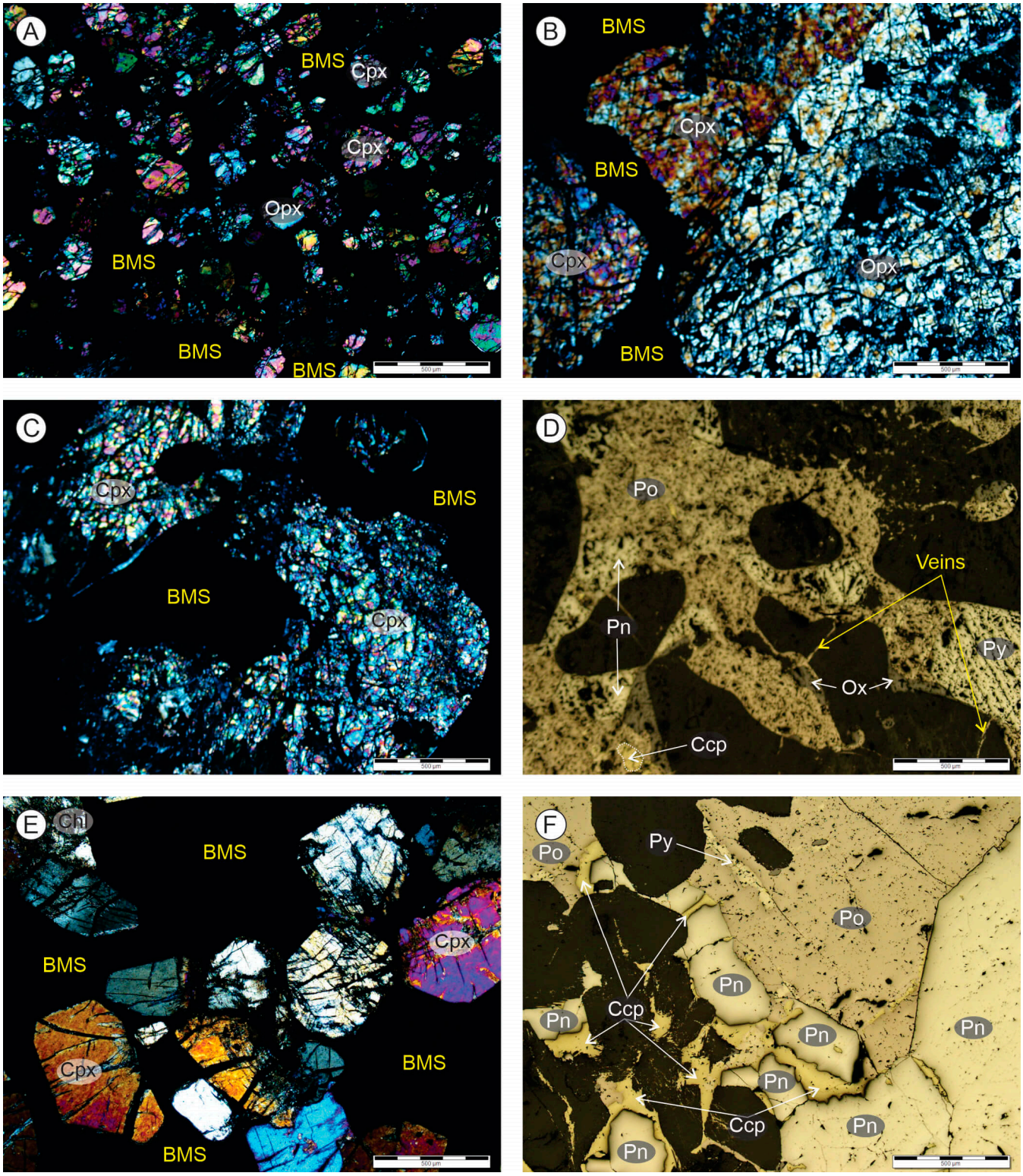

Figure 5. Photomicrographs of the high-grade semi-massive (**A**–**C**) and medium-grade semi-massive (**D**–**F**) sulfide ores show various silicates and sulfides. The scale bar at the bottom right corner of the images represents 500 µm. Refer to Figure 2 for explanation of the mineral abbreviations.

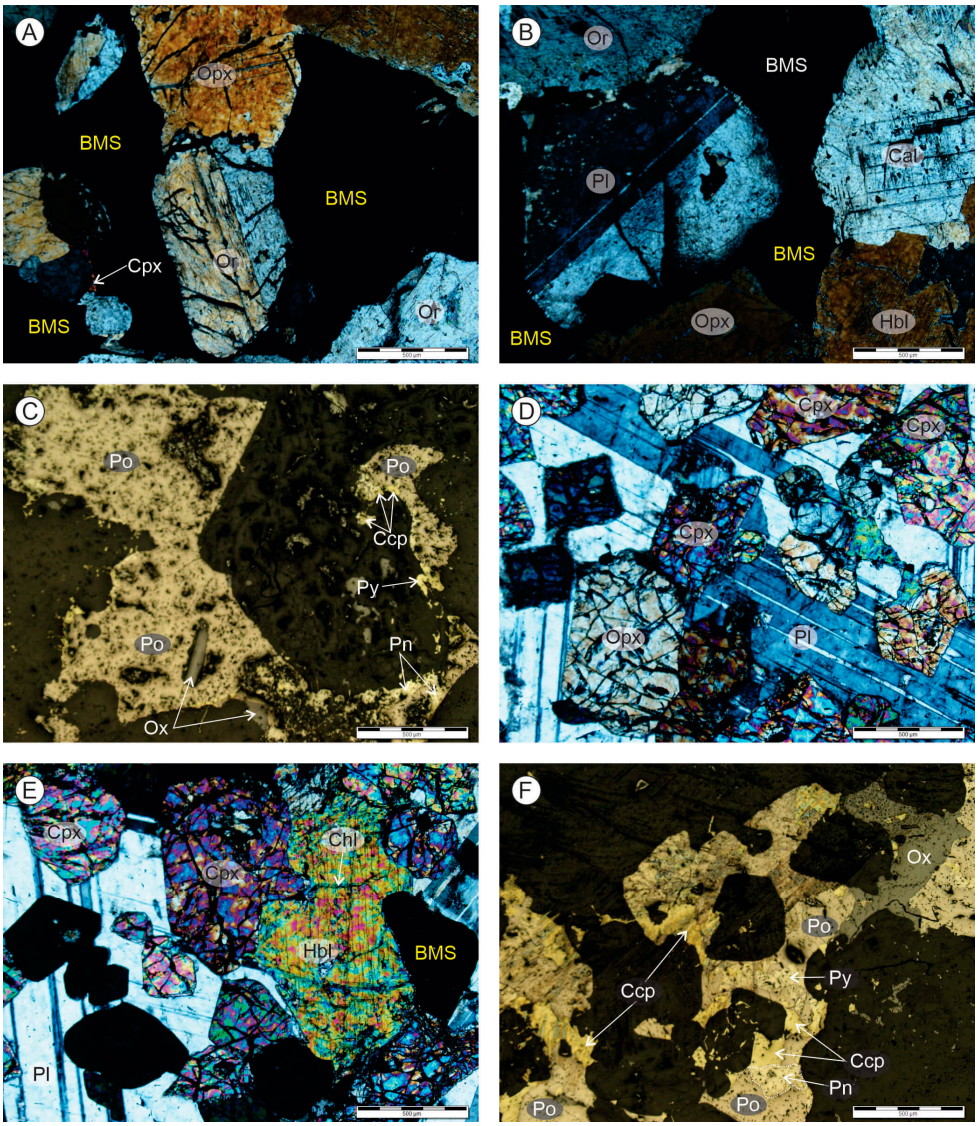

Figure 6. Photomicrographs of the high-grade net-texture ore (**A**–**C**) and medium-grade net-texture ore (**D**–**F**) showing various silicate and sulfide minerals. The scale bar at the bottom right corner of the images represents 500 µm. Refer to Figure 2 for explanation of the mineral abbreviations.

Table 3. Microscopic (petrographic) description of the PCMZ ores.

Ore Type	Mineralogical and Petrographic Description
Disseminated chromite-rich sulfide ore (PCMZ_MG&HG)	Consists of large poikilitic orthopyroxene crystals, which enclose some clinopyroxene and chlorite (Figure 7A,B,D,E). The pyroxenes are highly fractured and also altered on edges and within the fractures to form chlorite. The composite sulfides and chromite are disseminated within the silicate grain boundaries (Figure 7C,F,G). The composite sulfides consist of chalcopyrite, pentlandite, pyrrhotite, and pyrite. The chromite grains are also highly fractured, and some of the chromite cracks are filled with sulfides to form veins.
Massive chromitite ore (MCHR)	Consists of mainly fine chromite, with angular and rounded grains. The chromite grains are located predominantly within a matrix of chlorite, which forms a network around the chromite grains (Figure 8A,B). Olivine and serpentine are also present in minor amounts. Some of the chromite grains are fractured (Figure 8B). Trace sulfide minerals are also observed. The disseminated sulfide ore contains coarser grains of silicate, sulfides, and chromite minerals (Figure 7) than the massive chromite ore (Figure 8).

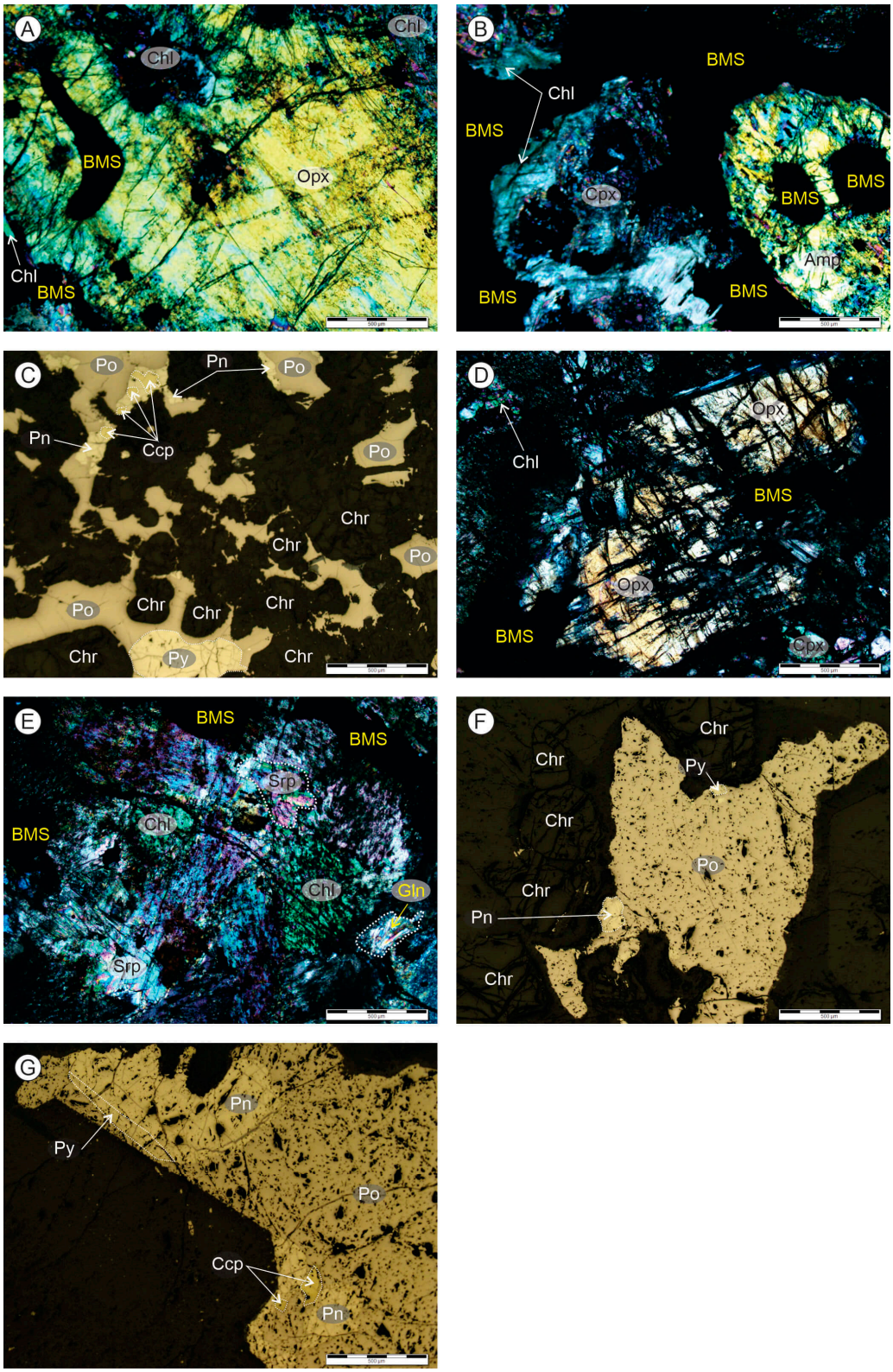

Figure 7. Photomicrographs of disseminated chromite-rich sulfide ore from the Peridotitic Chromitite Mineralized Zone showing various silicates (**A**,**B**,**D**,**E**), sulfides, and chromite (**C**,**F**,**G**). The scale bar at the bottom right corner of the images represents 500 µm. Refer to Figure 2 for explanation of the mineral abbreviations.

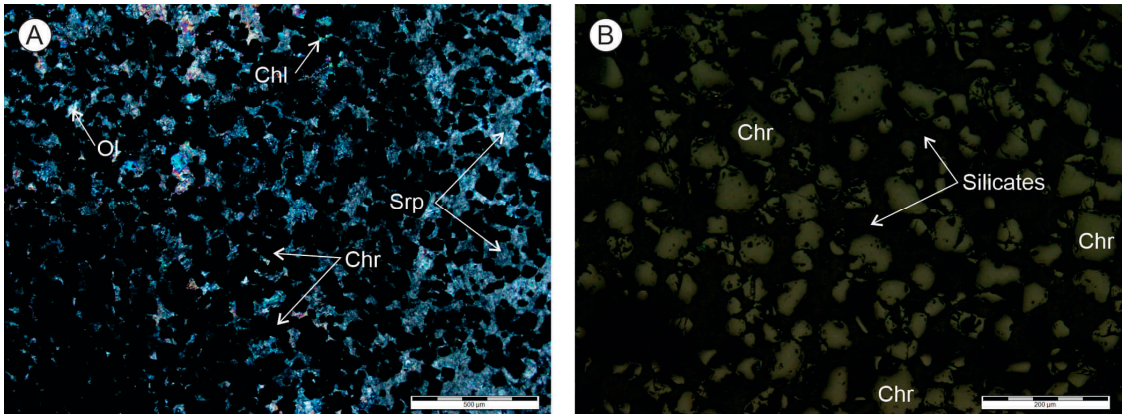

Figure 8. Photomicrographs of massive chromite ore from the Peridotitic Chromitite Mineralized Zone showing various silicate minerals and chromite. (**A**) Chlorite and serpentine forming networks around chromite grains; (**B**) Olivine, serpentine, and chlorite forming networks around chromite grains. The scale bar at the bottom right corner of the image represents 500 µm. Refer to Figure 2 for explanation of the mineral abbreviations.

4.3. Quantitative Mineralogy

The modal mineralogy of the various MMZ and PCMZ ore types are as per Table 4. The MS_MG ore variant contains lower amounts of altered silicates than the MS_HG ore variant. Clinopyroxene (12–46%) and orthopyroxene (up to 30%) are the dominant silicate minerals in all of the samples from the MMZ and PCMZ (Table 4). Pyrrhotite (4–63%) is the most abundant base metal sulfide, with minor quantities of pyrite (up to 10%), pentlandite (up to 7%), and chalcopyrite (up to 1.7%) in the ores from the MMZ. The ore samples from the PCMZ have the most abundant chromite (9–63%) and the least sulfides (Table 4).

Table 4. Mineral modal abundances of samples of the MMZ and PCMZ ore horizons (area % for ore crushed to −2 mm).

Mineral	BlebMG	BlebHG	DisMG	DisHG	MSMG	MSHG	SMSMG	SMSHG	NetMG	NetHG	PCMZMG	PCMZHG	MCHR
Actinolite	2.27	2.14	1.94	1.57	0.36	0.39	0.70	1.07	1.33	1.45	1.32	1.26	0.49
Amphibole	4.74	6.40	4.08	10.58	0.30	0.80	0.49	1.78	2.30	1.01	7.13	8.27	1.95
Biotite	0.35	0.43	0.49	0.71	0.14	0.20	0.29	0.35	0.44	0.31	0.26	0.23	0.54
Dolomite	0.56	0.79	0.53	0.76	0.09	0.10	0.12	0.71	0.21	0.10	0.50	0.68	0.50
Chalcopyrite	0.53	0.51	0.45	0.41	0.49	1.68	0.56	1.50	0.50	0.97	0.56	0.63	0.04
Chlorite	4.92	11.59	4.97	18.63	0.55	0.80	0.85	2.48	1.40	0.88	4.52	4.38	15.52
Chromite	1.14	0.56	0.06	0.55	0.02	0.01	0.01	0.01	1.93	0.01	22.85	9.65	63.35
Clinopyroxene	34.20	24.57	46.21	18.02	14.2	12.3	31.39	30.86	33.02	22.05	26.16	17.28	0.64
Olivine	0.27	0.47	0.14	0.48	0.04	0.04	0.02	0.11	0.16	0.08	0.52	0.66	1.17
Plagioclase	3.76	2.25	8.34	3.28	1.51	3.11	6.47	5.14	9.55	9.77	1.61	1.54	0.55
Orthopyroxene	24.79	30.48	21.8	24.49	1.81	3.17	3.65	11.84	29.42	21.76	24.41	36.31	0.45
Pentlandite	1.47	1.49	0.74	1.13	6.28	6.95	4.11	3.69	1.22	3.13	1.06	2.08	0.05
Pyrite	2.23	0.76	1.75	0.42	6.72	9.87	2.72	4.17	0.34	1.10	0.26	0.86	0.68
Pyrrhotite	13.66	11.98	4.16	10.85	63.97	56.65	44.27	30.24	12.88	31.99	5.13	9.98	0.03
Serp and Talc	0.45	0.38	0.31	0.11	0.06	0.01	0.13	0.23	0.68	0.16	1.01	2.67	1.14
Other	4.66	5.21	4.01	8.02	3.45	3.91	4.23	5.82	4.61	5.22	2.71	3.51	12.88
Total	100	100	100	100	100	100	100	100	100	100	100	100	100

4.4. Sample Assay

Nickel contents in the samples of the massive sulfide ore type vary from 3% to 3.5%, in the semi-massive sulfide ore type vary from 1.8% to 1.9%, and up to 1.7% in the high-grade net-textured sulfide ore type and the high-grade disseminated sulfide ore type (Table 5). The Bleb_MG/HG, Dis_MG/HG, NET-MG, and PCMZ_MG/HG are characterized by elevated magnesium contents on the order of 10–16% MgO; whilst the Dis_MG and NET_MG/HG

ores have the highest Ca content, which ranges from 4% to 8% CaO. The MS_MG/HG and PCMZ_MG/HG ores have the lowest Ca content, ranging up to 3% CaO.

Table 5. Sample assay.

Element	Fe	Mg	Ca	Al	S	Cu	Ni	Co	Cr
Unit	**wt%**	**wt%**	**wt%**	**wt%**	**wt%**	**ppm**	**ppm**	**ppm**	**ppm**
DL	**0.01**	**0.02**	**0.1**	**0.01**	**0.05**	**1**	**1**	**1**	**50**
Bleb_MG	14.80	11.70	6.33	2.22	6.24	2123	6690	334	6231
Bleb_HG	12.34	15.10	4.40	3.14	4.22	2333	5664	277	2745
Dis_MG	10.61	11.37	8.10	2.97	2.57	2035	3337	172	1941
Dis_HG	13.78	14.54	3.83	4.86	5.03	1758	6270	311	3172
SMS_MG	29.92	4.43	5.87	1.96	17.92	3206	19,424	966	1499
SMS_HG	26.34	6.64	5.73	1.76	15.95	6533	17,809	1036	1483
MS_MG	44.30	2.15	2.73	0.64	28.95	1761	26,300	1461	978
MS_HG	41.92	2.51	2.67	1.41	27.90	6558	29,400	2118	1211
Net_MG	18.79	10.55	5.50	2.33	6.42	2378	7033	382	9735
Net_HG	26.89	6.65	4.27	2.48	13.97	4775	17,249	738	1979
PCMZ_MG	14.29	12.15	2.90	4.08	2.61	2066	5043	290	10.22 wt%
PCMZ_HG	14.77	13.21	2.03	2.04	5.81	3211	10,478	465	2.84 wt%
MCHR	8.05	11.84	0.30	6.30	0.45	446	1719	117	35.97 wt%

4.5. Size Distribution of Pentlandite

The MS_HG and SMS_HG sulfide ore variants are characterized by the coarsest pentlandite, while the MCHR ore types have the smallest pentlandite (Figure 9). The remaining ore types have intermediate pentlandite grain size distributions, of relatively narrow range.

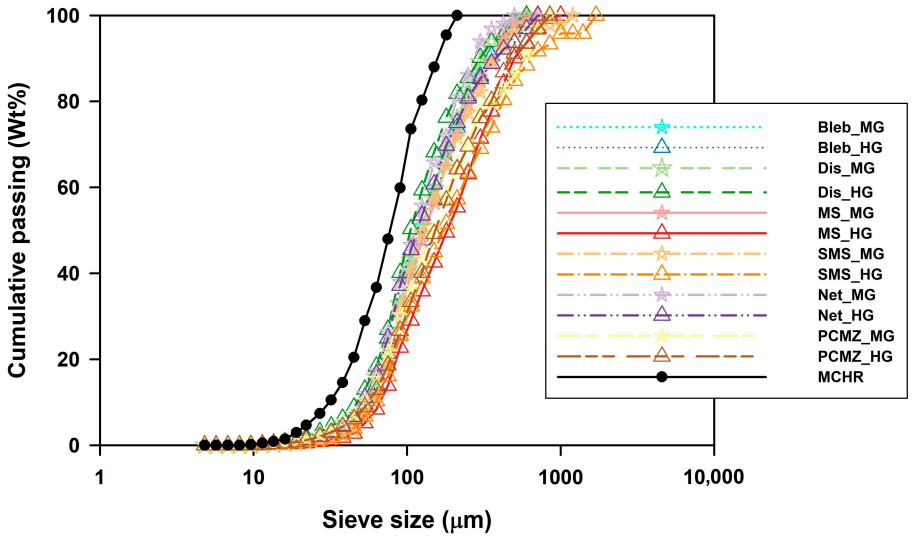

Figure 9. Pentlandite grain size distributions (equivalent circle diameter) for the samples of the various ore types collected from the MMZ and the PCMZ (crushed to −2 mm).

5. Sample Milling and Flotation

5.1. Milling Tests

The samples collected of the various ore types from the MMZ and the PCMZ differ substantially in their milling behavior (Figure 10), in that a wide range of milling times are required in order to reduce the various samples to e.g., a P67 of 75 micron (Figure 10). The high-grade ore varieties of the MMZ (with the exception of the MS_HG ore variety) as well as the PCMZ generally requires longer milling times than the medium-grade varieties.

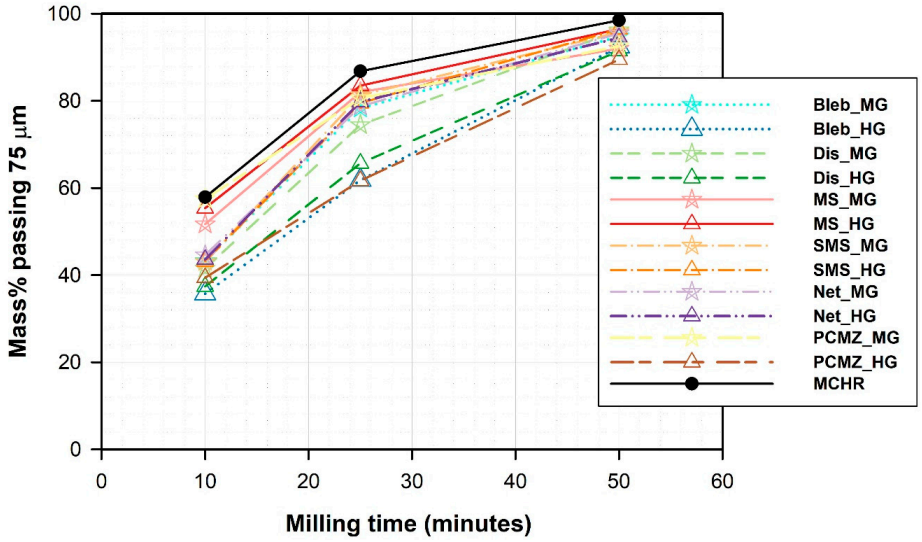

Figure 10. Cumulative mass % passing 75 µm sieve as a function of milling time for samples of the different ore textures collected from the MMZ and the PCMZ.

The Bleb_HG and Dis_HG sulfide ore textural variants of the MMZ requires the longest milling times for e.g., a P67 of 75 micron, while the massive sulfide ore variants require the shortest milling time (Figure 10).

The MCHR ore type of the PCMR ore horizon mills the fastest of all of the ore types investigated (Figure 10).

The liberation of pentlandite in the −75 + 38 micron sieve fraction of the mill product from the milling tests, as per Figure 11, is broadly similar (with the exception of the MCHR sample, which shows very poor liberation of pentlandite compared to all of the other samples investigated). The MG and HG samples of the PCMZ ore horizon are characterized by a somewhat lower level of pentlandite liberation, relative to the samples of the MMZ (Figure 11).

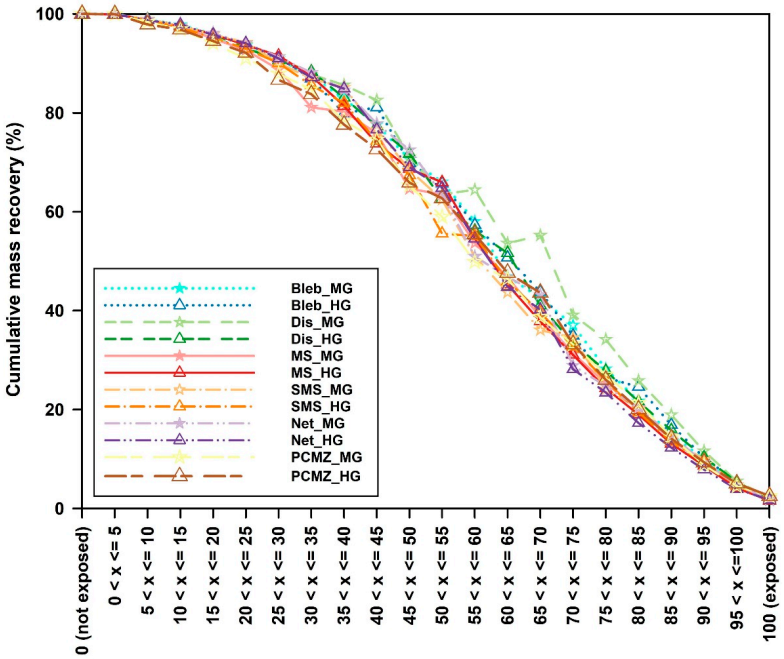

Figure 11. Cumulative liberation yield of pentlandite (weight %) in the −75 + 38 fractions of feed in the different grind sizes for high- and medium-grade variants of the sulfide ores from the MMZ and the PCMZ.

5.2. Flotation Tests

The flotation efficiency of the various ore types investigated in the present study, for grinds of P57, P67, and P77 at 75 µm (MMZ ore horizon), as well as P70, P80, and P90 at 75 micron (PCMZ ore horizon), is measured using cumulative recovery as a function of total flotation time (Figure 12), as well as concentrate grade as a function of cumulative Ni recovery (Figure 13).

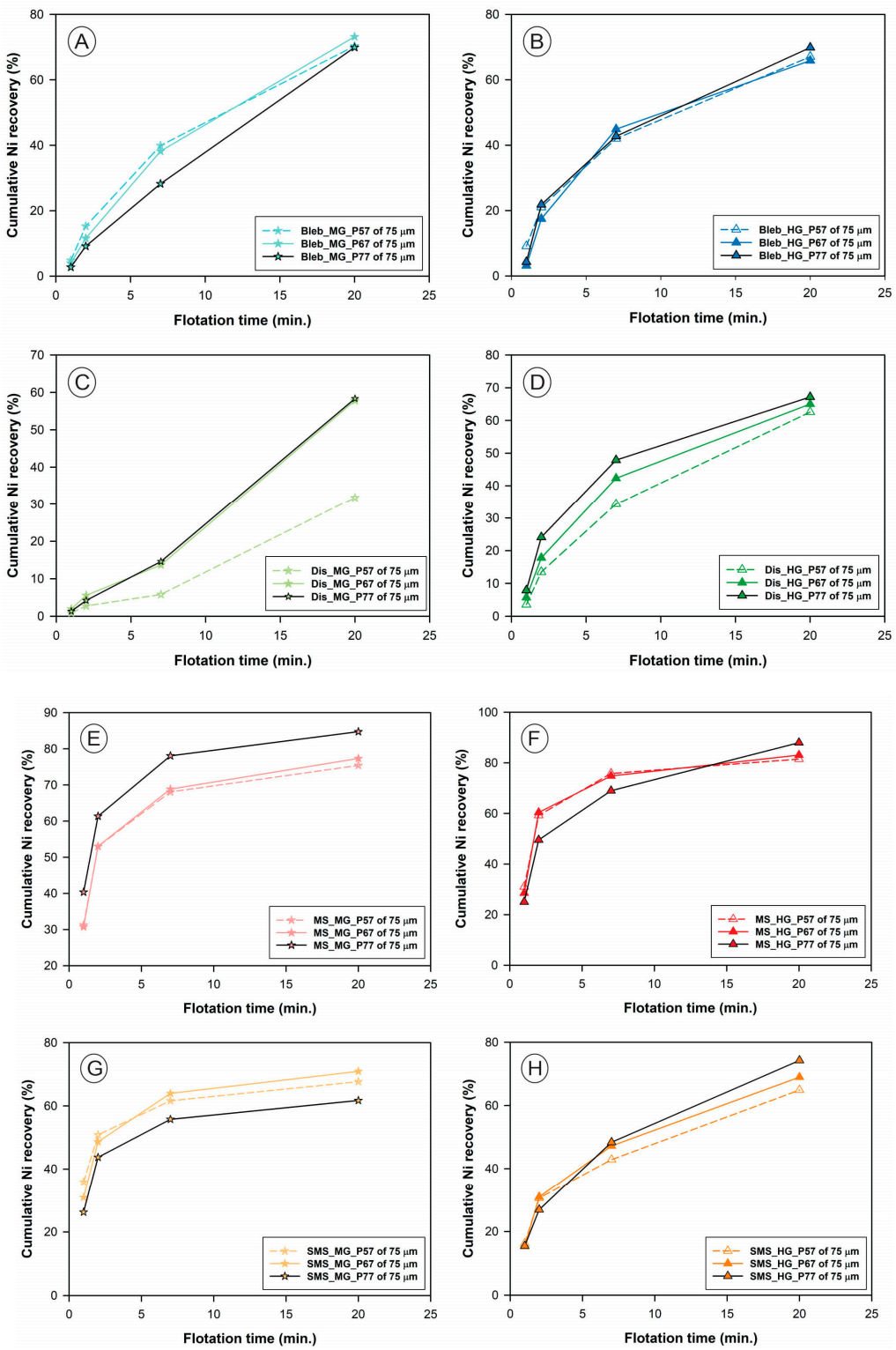

Figure 12. *Cont.*

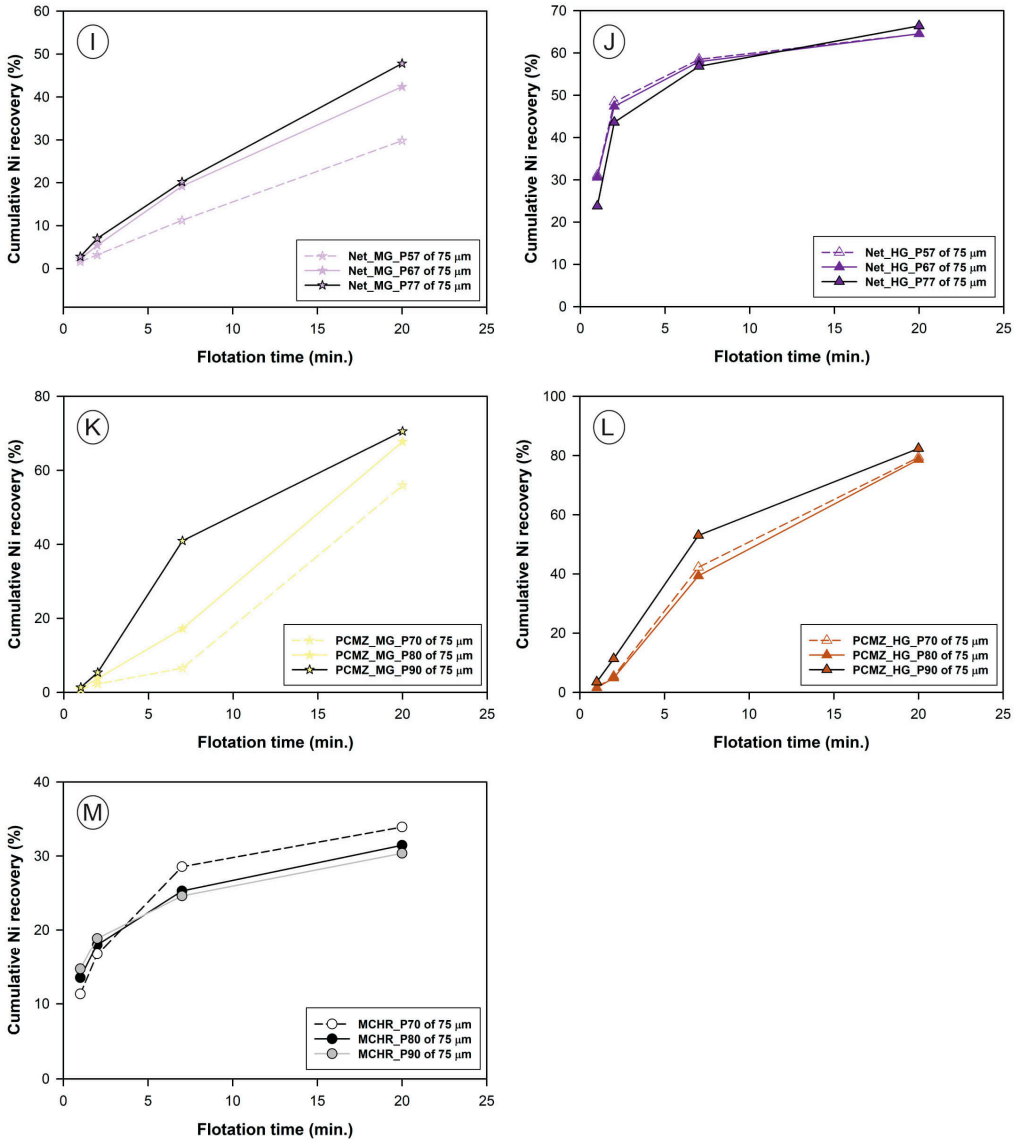

Figure 12. Cumulative Ni recovery as a function of flotation time for the flotation of the various ore types at the Nkomati Ni mine, milled to a grind of P57, P67, and P77 at 75 micron ((**A**–**J**) MMZ ore horizon)) as well as a grind of P70, P80, and P90 of 75 micron ((**K**–**M**) PCMZ ore horizon).

The results are highly variable. Generally, the finer grind sizes result in a higher abundance of floatable Ni-containing (pentlandite) particles, as shown by the higher cumulative Ni recoveries for P77 at 75 µm (MMZ) and P90 at 75 µm (PCMZ) (Figures 12 and 13).

A grind size of P77 at 75 µm results in the highest overall cumulative nickel recoveries for all of the sulfide ore textures from the MMZ, with the exception of the Bleb_MG sulfide ore variant, as well as the SMS_MG sulfide ore variant, which are characterized by the best Ni recoveries at a grind of P67 at 75 µm (Figures 12A,G and 13A,G).

A grind size of P90 at P75 µm, for samples from the PCMZ ore horizon, yields the best nickel recoveries in the PCMZ_MG and PCMZ_HG sulfide ores from the PCMZ (Figures 12K,L and 13K,L). In contrast, a grind size of P70 at 75 µm results in the best nickel recovery for the MCHR ore type of the PCMZ ore horizon (Figures 12M and 13M).

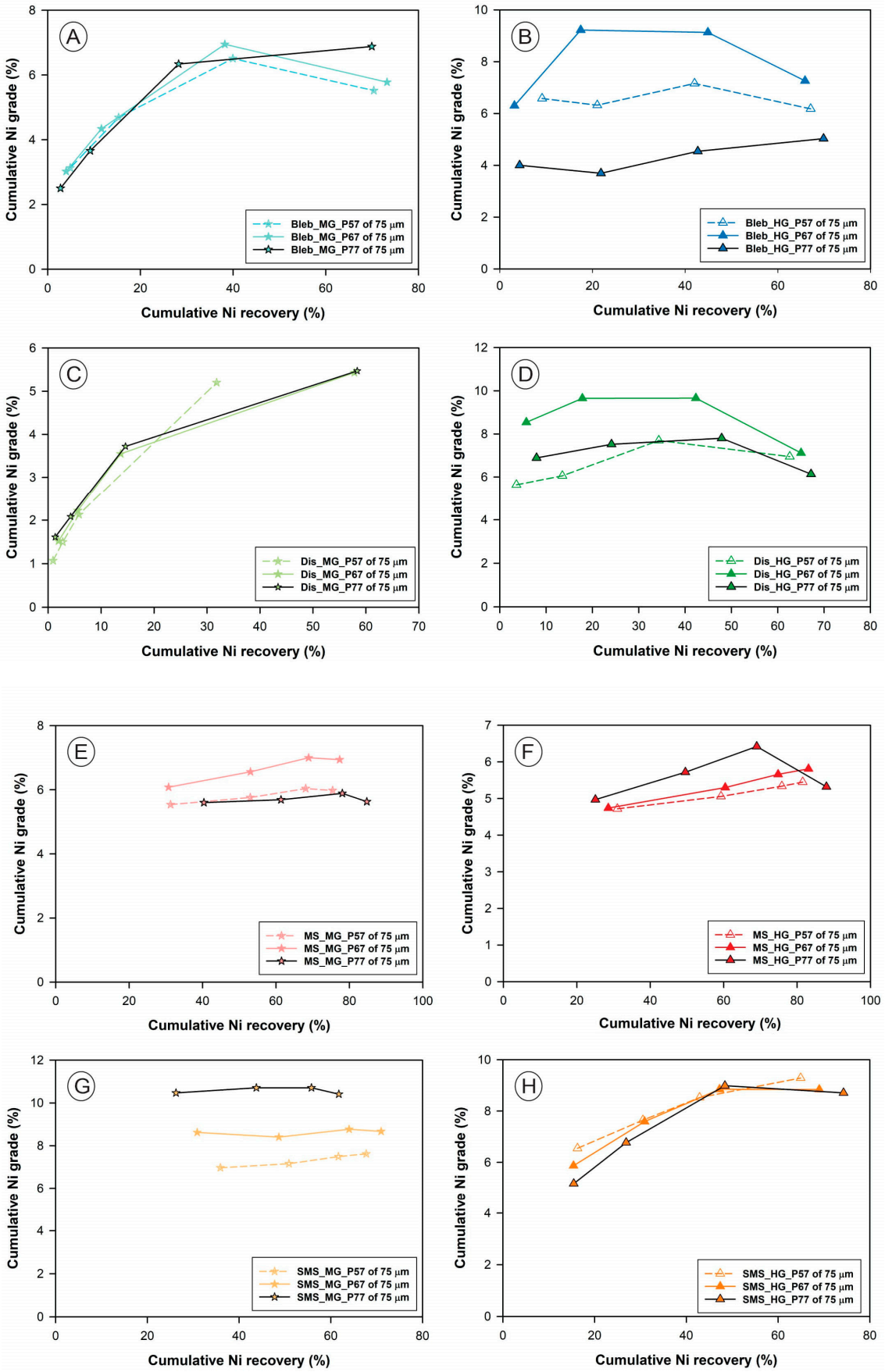

Figure 12. *Cont.*

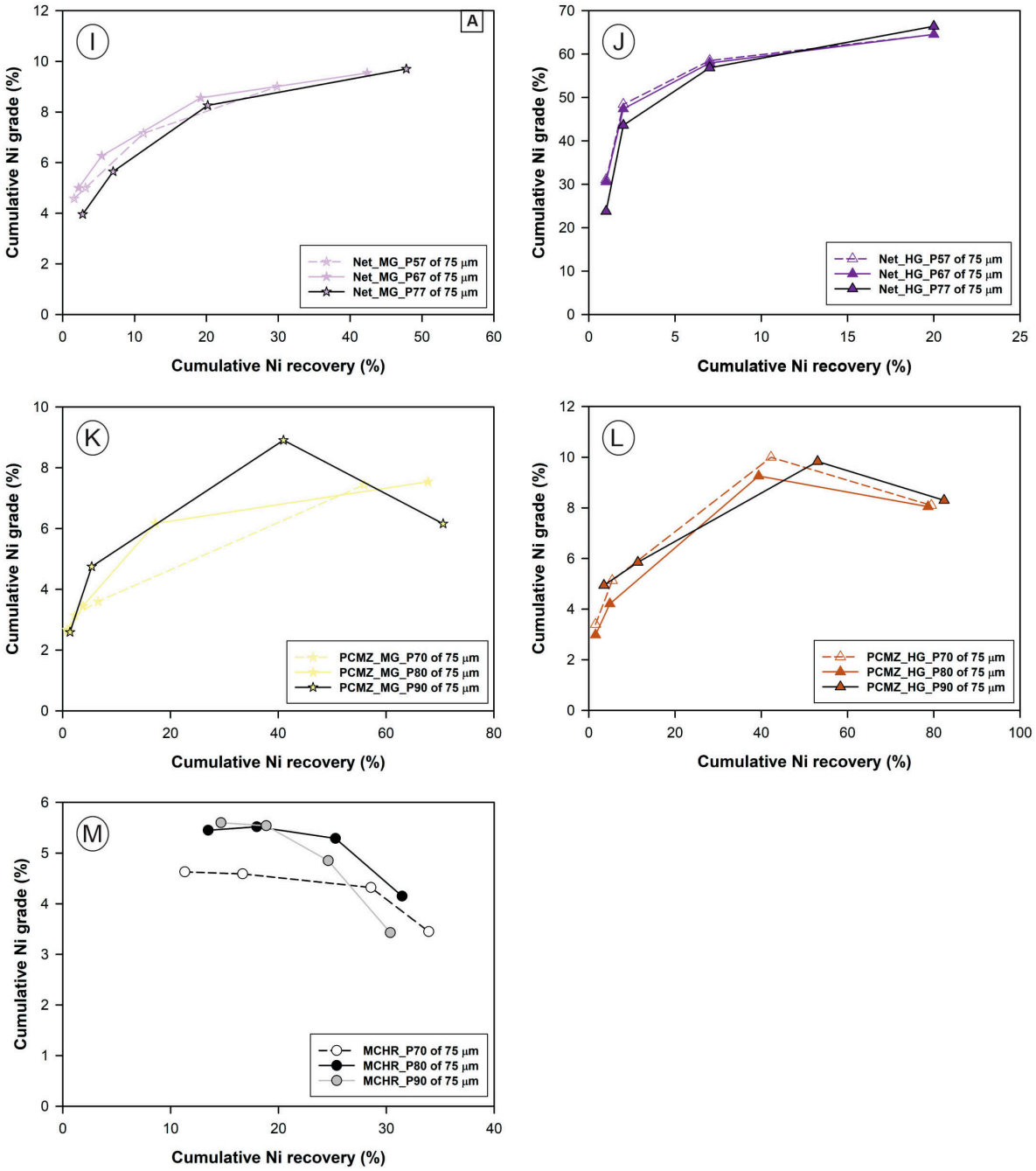

Figure 13. Cumulative concentrate grade vs. cumulative Ni recovery for the flotation of the various ore types at the Nkomati Ni mine, milled to a grind of P57, P67, and P77 at 75 micron ((**A**–**J**) MMZ ore horizon) as well as a grind of P70, P80, and P90 at 75 micron ((**K**–**M**) PCMZ ore horizon).

6. Discussion

The milling behavior of the Bleb_HG and Dis_HG ore variants from the MMZ correlates positively with the increasing modal abundances of pyroxene (particularly orthopyroxene at 24–31%), and correlates negatively with the increasing modal abundances of sulfides, especially pyrrhotite (Table 4; Figure 10). This trend is also observed in the chromite-rich sulfide ores of the PCMZ ore horizon, in which the PCMZ_HG ore type (36% orthopyroxene) requires the longest milling times (31–40 min) and the MCHR ore (0.5% orthopyroxene, but with 63% chromite) requires the shortest milling times (15–30 min) to achieve the required grinds (Figure 10), which by inference also means that the abundance of chromite has a major effect on milling times (i.e., ores mill faster with abundant chromite).

However, the modal abundances and hardness of (ortho)pyroxene alone cannot adequately explain the longer milling times required. For example, the net-textured sulfide ores with higher orthopyroxene content (22–29% orthopyroxene) require less milling time (15–23 min) than the Bleb_MG and Dis_MG sulfide ores (15–27 min). The difference in milling times can, therefore, also be attributed to the differences in ore texture and level of mineral alteration [21,24,49–51].

The Bleb_MG/HG, Dis_MG/HG, Net-MG, and PCMZ_MG/HG are characterized by high magnesium content, while the Dis_MG and Net_MG/HG ores have the highest Ca content, and the MS_MG/HG and PCMZ_MG/HG ores have the lowest. This is a function of the modal mineralogy, and correlates with the abundance of Ca-and Mg-bearing silicate minerals in these ores (Table 1). The mineralogy and the associated high Ca- and Mg-contents tend to have some downstream effects on the smelting of the concentrates when these minerals report to concentrate [23,24,52,53]. In such instances, the amine functional group-based depressants could be used to depress excessive fine-milled MgO-containing gangue minerals, as well as liberated pyrrhotite [54].

The mass pulls during flotation progressively increased with milling, and this can be attributed to the generally observed, increasing cumulative liberation yields of sulfides, including pentlandite, as milling progressed in all of the ores from the MMZ and PCMZ (Figure 12), as also observed previously for Nkomati, and elsewhere [20,33,55,56]. The mass pulls are highest in the samples with the most abundant sulfides (MS and SMS; and Net_MG and Net_HG sulfide ores; and PCMZ_MG and PCMZ_HG ores) due to the higher floatability tendency of sulfides when compared to silicate and oxide (chromite) minerals (Figure 12; Table 4). Orthopyroxene, though known to be readily floatable, appears to contribute little to the observed mass pulls in this case [57].

The grind of P77 at 75 µm produced the most superior nickel recoveries in all of the sulfide ore types from the MMZ, which is likely a result of the increased pentlandite liberation in this grind size [28,33,37,55,56,58]. However, the Bleb_MG sulfide ore and the SMS_MG sulfide ore are an exception, and which resulted in the highest Ni recovery in the P67 at 75 µm grind. This could be due to poor pentlandite recovery in the P77 at 75 µm grind size in these specific ore variants [23,32,44,52,53].

A grind of P90 at 75 µm also yielded the best nickel recovery values in the PCMZ_MG and PCMZ_HG ore variants from the PCMZ, except in the MCHR ore, in which the P70 at 75 µm grind produced the best nickel recovery value. The overall implication of these outcomes is that the P77 at 75 µm grind size would be the optimum grind size for milling all of the sulfide ore types mined from the MMZ, to yield the best liberation of pentlandite and the best overall nickel recoveries. The P90 at 75 µm and P70 at 75 µm grinds would be ideal to produce the best nickel recoveries from the PCMZ_MG and PCMZ_HG ores, and the MCHR ores, respectively. However, for all practical purposes, due to the inadequacy of a single ore type to meet the daily run of mine ore requirements, a grind of P80 at 75 µm would be ideal for processing all of the ores as a composite [27].

The highest nickel grades produced by the P77 at 75 µm grind in the Bleb_MG, Dis_MG, SMS_MG, Net_MG, and Net_HG sulfide ores; and by the P67 at 75 µm grind in the Bleb_HG, the Dis_MG, and the Dis_HG sulfide ores, as well as the MS_MG sulfide ore (Figure 13) are consistent with the lower mass pulls produced in these grinds. The P80 at 75 µm grind also produced the highest nickel grades in the PCMZ_MG sulfide ore and the MCHR ore, and this is also in agreement with the lower mass pulls achieved by this grind in these ores.

7. Conclusions

The following conclusions are drawn from this study:

(1) The modal abundances of orthopyroxene and sulfides; and the orthopyroxene and chromite in the ores of the MMZ and the PCMZ, respectively, and ore texture, have a direct influence on the milling time requirements and the amount of energy required to produce the required grinds passing 75 µm. Longer milling times are required for

the ores with higher abundances of orthopyroxene and fewer sulfides for the ores from the MMZ, while longer milling times are also required for the ores of the PCMZ with higher abundances of orthopyroxene and less chromite. Ore blending prior to milling could limit the amount of orthopyroxene and increase the sulfides' abundance, thereby reducing the milling times, and ultimately the energy consumption of the milling circuits;

(2) The positive correlation of high mass pulls with high sulfides' abundances indicate that such elevated abundances are necessary for the flotation-based recovery of Ni. Orthopyroxene, though known to be readily floatable, appears to contribute little to the observed mass pulls;

(3) The P77 at 75 μm grind produces the best nickel recovery in the ores from the MMZ, while the P90 at 75 μm, and the P70 at 75 μm grinds yields the best nickel recoveries in the PCMZ_MG and PCMZ_HG sulfide ores from the PCMZ, respectively. These higher Ni recoveries in the finest grinds, are consistent with increased cumulative mass pulls and cumulative liberation yields of pentlandite with progressive milling. It should, though, be considered that the application of the P77 and P90 at 75 μm grinding levels may impact negatively on the energy consumption of the milling circuits. However, for all practical purposes, due to the inadequacy of a single ore type to meet the daily run of mine ore requirements, grinds of P77 at 75 μm and P80 at 75 μm would be ideal for processing ores as a composite from the MMZ and the PCMZ, respectively;

(4) The P77 at 75 μm grind produced the highest nickel grades in the Bleb_MG, Dis_MG, SMS_MG, Net_MG, and Net_HG ore variants of the MMZ, while the P67 at 75 μm grind produced the highest nickel grades in the Bleb_Hg, Dis_MG, Dis_HG, and MS_MG ores of the MMZ, and the P80 at 75 μm grind produced the highest nickel grades in the PCMZ_MG and the MCHR ores of the PCMZ. This is in agreement with the lower mass pulls achieved by these grinds in these ores. Therefore, a grind of P77 at 75 μm, as well as a grind of P80 at 75 μm, would be expected to yield the best overall Ni recoveries and grades in the sulfide ores from the MMZ and the PCMZ, respectively.

8. Recommendations

The following recommendations are worth considering:

1. The sulfide ores from the MMZ could be milled at a grind of P77 at 75 μm to produce optimal yields of cumulative liberated pentlandite, and to yield the best overall Ni recovery and grades of up to 88% and 12%, respectively (Figures 12 and 13), instead of the grind of P67 at 75 μm currently in use at the Nkomati mine;
2. The PCMZ ores which achieved overall recovery and grade values of up to 79% and 8%, respectively, at a grind of P80 at 75 μm, and the MMZ ores which yielded best Ni and grade values of up to 88% and 12% at a grind of P77 at 75 μm, could potentially be blended and milled together at a grind of P80 at 75 μm to achieve optimum recoveries and grades in a single circuit;
3. A combination of flotation to recover sulfides within floatable particle sizes and gravity separation to recover liberated sulfides which are beyond floatable sizes and have reported flotation tailings especially for the MS_MG and MS_HG, as well as the SMS_MG and SMS_HG ore variants at the current grind size of P67 at 75 μm grind could be used. This could be followed by regrinding and flotation of the gravity sulfide concentrates to increase overall Ni recoveries, especially in the MS_MG and MS_HG ore variants, as well as the SMS_MG and SMS_HG ore variants;
4. More efficient and effective flotation circuits to recover the fine sulfide mineral particles from a single finer target grind size of P77 at 75 μm could also be designed and employed, or flotation reagents' optimization could be employed to recover any fine pentlandite particles that could potentially be lost to tailings;

5. Staged grinding to produce optimal floatable particle sizes and reduce excessive fine sulfide particles, followed by flotation, would likely improve the recovery of the valuable minerals. Staged grinding would also reduce the excessive production of the undesirable Ca- and Mg-rich minerals that are detrimental to downstream processing (resulting in high MgO and CaO contents in flotation products), especially for the Bleb_MG/HG, Dis_MG/HG, Net-MG, and PCMZ_MG/HG with elevated magnesium contents, and the Dis_MG and Net_MG/HG ore with elevated Ca contents. This would strike a balance between size reduction and optimal recoverability of the valuable minerals. Amine-based depressants could also be used to depress excessive fine-milled MgO-containing gangue minerals and liberated pyrrhotite.

Author Contributions: Conceptualization, T.D. and F.V.; methodology, T.D. and D.H.R.; software, T.D. and D.H.R.; validation, T.D., F.V., N.C. and D.H.R.; formal analysis, T.D., F.V., N.C. and D.H.R.; investigation, T.D., F.V., N.C. and D.H.R.; resources, T.D., F.V., N.C. and D.H.R.; data curation, N.C. and T.D.; writing—original draft preparation, T.D., F.V., N.C. and D.H.R.; writing—review and editing, T.D., F.V., N.C. and D.H.R.; visualization, T.D., F.V., N.C. and D.H.R.; supervision, F.V., N.C. and D.H.R.; project administration, T.D., F.V., N.C. and D.H.R. All authors have read and agreed to the published version of the manuscript.

Funding: This research was funded by the SA Department of Science and Innovation through their Research Chairs Initiative (Geometallurgy), as administered by the National Research Foundation (Grant Number 64779 to Fanus Viljoen).

Institutional Review Board Statement: Not applicable.

Informed Consent Statement: Not applicable.

Data Availability Statement: Data supporting reported results can be provided from authors upon request.

Acknowledgments: The authors would like to express their gratitude to Nkomati Mine management for allowing access to their operation to collect samples and to Senmin (Richard Bergmann) for supplying reagents used in this study. Fanus Viljoen acknowledges funding from the South African Department of Science and Innovation Research Chairs Initiative, as administered by the National Research Foundation. The DSI-NRF Centre of Excellence for Integrated Mineral and Energy Resource Analysis (CIMERA) at the University of Johannesburg is also acknowledged for general funding of a geometallurgical nature.

Conflicts of Interest: The authors declare no conflict of interest.

References

1. Farrar, J.C.M. *The Alloy Tree—A Guide to Low-Alloy Steels, Stainless Steels and Nickel Base Alloys*; Woodhead Publishing Limited: Cambridge, UK, 2004; p. 192.
2. Starostin, V.I.; Sorokhtin, O.G. A new interpretation for the origin of the Norilsk type PGE-Cu-Ni sulfide deposits. *Geosci. Front.* **2011**, *2*, 583–591. [CrossRef]
3. Naldrett, A.J. World-class Ni-Cu-PGE deposits: Key factors in their genesis. *Miner. Depos.* **1999**, *34*, 227–240. [CrossRef]
4. Don, H.R.; John, S.F.; Burkhard, O.D. Sudbury Breccia (Canada): A product of the 1850 Ma Sudbury Event and host to footwall Cu–Ni–PGE deposits. *Earth-Sci. Rev.* **2003**, *60*, 147–174.
5. Hoatson, D.M.; Jaireth, S.; Jaques, A.L. Nickel sulfide deposits in Australia: Characteristics, resources, and potential. *Ore Geol. Rev.* **2006**, *29*, 177–241. [CrossRef]
6. Ashcroft, G. Nickel Laterites: The World's Largest Source of Nickel. Available online: https://www.geologyforinvestors.com/ (accessed on 12 June 2014).
7. Elias, M. Nickel laterite deposits—Geological overview, resources and exploitation. *CODES Spec. Publ.* **2002**, *4*, 205–220.
8. Van der Ent, A.; Baker, A.J.M.; Van Baglooy, M.M.J.; Tjoan, A. Ultramafic nickel laterites in Indonesia (Sulawesi, Halmahera): Mining, nickel hyperaccumulators and opportunities for phytomining. *J. Geochem. Explor.* **2013**, *128*, 72–79. [CrossRef]
9. Schouwstra, R.P.; Kinloch, E.D. A Short Geological Review of the Bushveld Complex. *Platin. Met. Rev.* **2000**, *44*, 33–39.
10. Song, X.; Wang, Y.; Chen, L. Magmatic Ni-Cu-(PGE) deposits in magma plumbing systems: Features, formation and exploration. *Geosci. Front.* **2011**, *2*, 375–384. [CrossRef]
11. Gauert, C. Sulfide and oxide mineralisation in the Uitkomst Complex, South Africa: Origin in a magma conduit. *J. Afr. Earth Sci.* **2001**, *32*, 149–161. [CrossRef]

12. Dominy, S.C.; O'Connor, L.; Parkhakar-Fox, A.; Glass, H.J.; Purevgerel, S. Geometallurgy—A Route to More Resilient Mine Operations. *Minerals* **2018**, *8*, 560. [CrossRef]
13. Gauert, C.D.K.; de Waal, S.A.; Wallmach, T. Geology of the ultrabasic to basic Uitkomst complex, eastern Transvaal, South Africa: An overview. *J. Afr. Earth Sci.* **1995**, *21*, 553–570. [CrossRef]
14. De Waal, S.A.; Maier, W.D.; Armstrong, R.A.; Gauert, C.D.K. Parental magma and emplacement of the stratiform Uitkomst Complex, South Africa. *Can. Mineral.* **2001**, *39*, 557–571. [CrossRef]
15. Hulley, V. Reactions between Country Rock Xenoliths and the Magma of the Uitkomst Complex, with Implications for the Origin of the Sulfide Mineralisation. Master's Thesis, University of Pretoria, Pretoria, South Africa, 2005.
16. Kenyon, A.K.; Attridge, R.L.; Coetzee, G.L. The Uitkomst Nickel-Copper deposit, Eastern Transvaal. *Miner. Depos. South. Afr.* **1986**, *v2*, 1009–1017.
17. Theart, H.F.J.; de Nooy, C.D. The Platinum Group Minerals in two parts of the Massive Sulfide Body of the Uitkomst Complex, Mpumalanga, South Africa. *S. Afr. J. Geol.* **2001**, *104*, 287–300. [CrossRef]
18. Dzvinamurungu, T. A Geometallurgical Investigation of the Main Mineralised Zone and the Peridotitic Chromitite Mineralised Zone at the Nkomati Mine, with a View on the Liberation and Recovery of Pentlandite and Chromite. Ph.D. Thesis, University of Johannesburg, Johannesburg, South Africa, 2017.
19. Dzvinamurungu, T.; Rose, D.H.; Viljoen, K.S.; Mulaba-Bafubiandi, A. A process Mineralogical Evaluation of Chromite at the Nkomati Nickel Mine, Uitkomst Complex, South Africa. *Minerals* **2020**, *10*, 709. [CrossRef]
20. Mishra, G.; Viljoen, K.S.; Mouri, H. Influence of Mineralogy and Ore Texture on Pentlandite Flotation at the Nkomati Nickel Mine, South Africa. *Miner. Eng.* **2013**, *54*, 63–78. [CrossRef]
21. Tomanec, R.; Cablik, V.; Simovic, I.; Gacina, R. Ore Microscopy Characterization as a Mineral Processing Control. *Inz. Miner.* **2014**, *15*, 101–106.
22. Evans, C.L.; Bradshaw, D.J. Modelling flotation recovery in geometallurgical programmes. In Proceedings of the 6th International Flotation Conference (Flotation'13), Cape Town, South Africa, 18–21 November 2013.
23. Johnson, N.W. Liberated 0–10 µm particles from sulphide ores, their production and separation—Recent developments and future needs. *Miner. Eng.* **2006**, *19*, 666–674. [CrossRef]
24. Becker, M.; Brough, C.; Reid, D.; Smith, D.; Bradshaw, D. Geometallurgical characterization of the Merensky Reef at Northam Platinum Mine—Comparison of Normal, Pothole and Transitional Reef types. In Proceedings of the Ninth International Congress of Applied Mineralogy, Brisbane, Australia, 8–10 September 2008; pp. 391–399.
25. Lotter, N.O. Modern Process Mineralogy: An integrated multi-disciplined approach to flowsheeting. *Miner. Eng.* **2011**, *24*, 1229–1237. [CrossRef]
26. Lotter, N.O.; Kormos, L.J.; Oliveira, J.; Fragomeni, D.; Whiteman, E. Modern Process Mineralogy: Two case studies. *Miner. Eng.* **2011**, *24*, 638–650. [CrossRef]
27. Van Tonder, E.; Deglon, D.A.; Napier-Munn, T.J. The effect of ore blends on the mineral processing of platinum ores. *Miner. Eng.* **2010**, *23*, 621–626. [CrossRef]
28. Lastra, R. Seven practical application cases of liberation analysis. *Int. J. Miner. Process.* **2007**, *84*, 337–347. [CrossRef]
29. Lotter, N.O.; Fragomeni, D. High-confidence flotation testing at Xstrat Process Support. *Miner. Metall. Process.* **2010**, *27*, 47–54.
30. Lotter, N.O.; Kowal, D.L.; Tuzun, M.A.; Whittaker, P.J.; Kormos, L. Sampling and flotation testing of Sudbury Basin drill core for process mineralogy modeling. *Miner. Eng.* **2003**, *16*, 857–864. [CrossRef]
31. Lotter, N.O.; Di Feo, A.; Kormos, L.J.; Fragomeni, D.; Comeau, G. Design and measurement of small recovery gains: A case study at Raglan concentrator. *Miner. Eng.* **2010**, *23*, 567–577. [CrossRef]
32. Lotter, N.O.; Whiteman, E.; Bradshaw, D.J. Modern practice of laboratory flotation testing for flowsheet development—A review. *Miner. Eng.* **2014**, *66*, 2–12. [CrossRef]
33. Young, M.F.; Pease, J.D.; Johnson, N.W.; Munro, P.D. Developments in Milling Practice at the Lead/Zinc Concentrator of Mount Isa Mines Limited from 1990. In Proceedings of the AusIMM Sixth Mill Operators Conference, Madang, Papua New Guinea, 6–8 October 1997; pp. 1–19.
34. Mulaba-Bafubiandi, A.F.; Medupe, O. An assessment of pentlandite occurrence in the run of mine ore from BCL Mine (Botswana) and its impact on the flotation yield. In Proceedings of the The Fourth Southern African Conference on Base Metals 2007—'Africa's metals resurgence', Swakopmund, Namibia, 23–27 July 2007; pp. 57–75.
35. Craig, J.R.; Vaughan, D.J. *Ore Microspcopy and Ore Petrography*, 2nd ed.; John Wiley & Sons: Hoboken, NJ, USA, 1994; pp. 331–332.
36. Craig, J.R. Ore-mineral textures and the tales they tell. *Can. Mineral.* **2001**, *39*, 937–956. [CrossRef]
37. Chryssoulis, S.L. Using Mineralogy to Optimize Gold Recovery by Flotation. *J. Mineral.* **2001**, *53*, 48–50. [CrossRef]
38. Liipo, J. Characterization of the mode of occurrence of gold in Jokisivu pilot feed and products. *Miner. Eng.* **2003**, *16*, 1317–1321. [CrossRef]
39. Gu, Y. Automated Scanning electron Microscope based Mineral liberation Analysis An introduction to JKMRC/FEI Mineral Liberation Analyser. *J. Miner. Mater. Charact. Eng.* **2003**, *2*, 33–41. [CrossRef]
40. Fandrich, R.; Gu, Y.; Burrows, D.; Moeller, K. Modern SEM-based mineral liberation analysis. *Int. J. Miner. Process.* **2007**, *84*, 310–320. [CrossRef]
41. Becker, M.; Harris, P.J.; Wiese, J.G.; Bradshaw, D.J. Mineralogical characterization of naturally floatable gangue in Merensky Reef ore flotation. *Int. J. Miner. Process.* **2009**, *93*, 246–255. [CrossRef]

42. Wiese, J.; Harris, P.; Bradshaw, D. The effect of the reagent suite on froth stability in laboratory scale batch flotation tests. *Miner. Eng.* **2011**, *24*, 995–1003. [CrossRef]
43. Muganda, S.; Zanin, M.; Grano, S.R. Benchmarking the flotation performance of ores. *Miner. Eng.* **2012**, *26*, 70–79. [CrossRef]
44. Senior, G.D.; Shannon, L.K.; Trahar, W.J. The flotation of pentlandite from pyrrhotite with particular reference to the effects of particle size. *Int. J. Miner. Process.* **1994**, *42*, 169–190. [CrossRef]
45. Francisco, T.; Mehdi, S.; David, D.; Laurindo, L.F. Influence of agitation intensity on flotation rate of apatite particles. *REM-Int. Eng. J.* **2017**, *70*, 491–495. [CrossRef]
46. Hassanzadeh, A.; Safari, M.; Hoang, D.H. Fine, Coarse and Fine-Coarse Particle Flotation in Mineral Processing With A Particular Focus On The Technological Assessments. In Proceedings of the 2nd International Electronic Conference on Mineral Science, Online, 1–15 March 2021.
47. Senior, G.D.; Trahar, W.J.; Guy, P.J. The selective flotation of pentlandite from a nickel ore. *Int. J. Miner. Process.* **1995**, *43*, 209–234. [CrossRef]
48. Wiese, J.; Harris, P.; Bradshaw, D. The influence of the reagent suite on flotation of ores from the Merensky reef. *Miner. Eng.* **2005**, *18*, 189–198. [CrossRef]
49. Lenahan, W.C.; de Murray-Smith, R.L. *Assay and Analytical Practice in the South African Mining Industry*; Monograph series M6; The South African Institute of Mining and Metallurgy: Johannesburg, South Africa, 1986; pp. 41–594.
50. Deer, W.A.; Howie, R.A.; Zussman, J. *An Introduction to the Rock forming Minerals*, 2nd ed.; Lonman: London, UK, 1992.
51. Hunt, J.; Berry, R.; Bradshaw, D. Characterising chalcopyrite liberation and flotation potential: Examples from an IOCG deposit. *Miner. Eng.* **2011**, *24*, 1271–1276. [CrossRef]
52. Runge, K.C.; Franzidis, J.P.; Manlapig, E.V. A study of the flotation characteristics of different classes in different streams of an industrial circuit. In Proceedings of the XXII International Mineral Processing Congress, Cape Town, South Africa, 29 September–3 October 2003; pp. 962–972.
53. Runge, K.; McMaster, J.; Ijsselsteijn, M.; Vien, A. Establishing the Relationship between Grind Size and Flotation Recovery using Modelling Techniques. In Proceedings of the Flotation 2007 Minerals Engineering Conference, Cape Town, South Africa, 6–21 November 2007.
54. Dai, Z.; Bos, J.; Lee, A.; Wells, P. Mass balance and mineralogical analysis of flotation plant survey samples to improve plant metallurgy. *Miner. Eng.* **2008**, *21*, 826–831. [CrossRef]
55. Yildirim, B.G.; Bradshaw, D.; Powell, M.; Evans, C.; Clark, A. Development of an effective and practical Process Alteration Index (PAI) for predicting metallurgical responses of Cu porphyries. *Miner. Eng.* **2014**, *69*, 91–96. [CrossRef]
56. Hay, M.P.; Roy, R. A case study of optimizing UG2 flotation performance. Part 1: Bench, pilot and plant factors which influence Cr_2O_3 entrainment in UG2 flotation. *Miner. Eng.* **2010**, *23*, 855–867. [CrossRef]
57. Ford, F.D.; Wercholaz, C.R.; Lee, A. Predicting process outcomes for Sudbury platinum group minerals using grade-recovery modelling from mineral liberation analyzer (MLA) data. *Can. Mineral.* **2011**, *49*, 1627–1642. [CrossRef]
58. Perez-Barnuevo, L.; Pirard, E.; Castroviejo, R. Automated characterization of intergrowth textures in mineral particles. A case study. *Miner. Eng.* **2013**, *52*, 136–142. [CrossRef]